Chemical Science

Accepted Manuscript

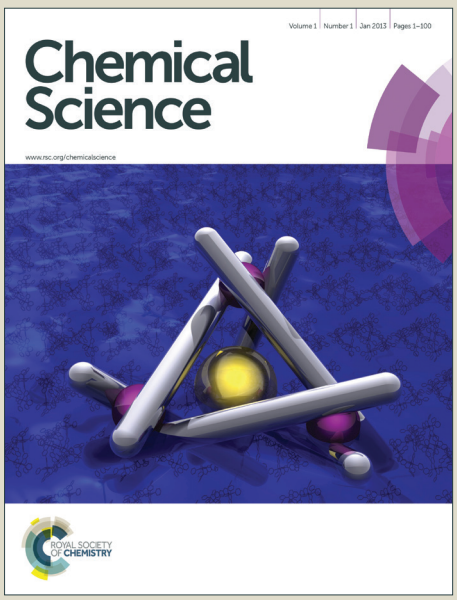

ROYAL SOCIETY OF CHEMISTRY

www.rsc.org/chemicalscience

Chemical Science

Cite this: DOI: 10.1039/c0xx00000x
www.rsc.org/xxxxxx

EDGE ARTICLE

Bodipy-C_{60} triple hydrogen bonding assembly as heavy atom-free triplet photosensitizers: preparation and study of the singlet/triplet energy transfer

Song Guo,[a] Liang Xu,[b] Kejing Xu,[a] Jianzhang Zhao,*[a] Betül Küçüköz,[c] Ahmet Karatay,[c] Gul Yaglioglu,[c] Mustafa Hayvali,[d] Ayhan Elmali [c]

Received (in XXX, XXX) Xth XXXXXXXXX 20XX, Accepted Xth XXXXXXXXX 20XX
DOI: 10.1039/b000000x

Supramolecular triplet photosensitizers based on hydrogen bonding-mediated molecular assemblies were prepared. Three thymine-containing visible light-harvesting Bodipy derivatives (**B-1**, **B-2** and **B-3**, which show absorption at 505 nm, 630 nm and 593 nm, respectively), were used as one of the H-bonding module, and 1,6-diaminopyridine appended C_{60} was used as the complementary hydrogen bonding module (**C-1**), in which the C_{60} part is as the spin converter for triplet formation. Visible light-harvesting antenna with *methylated* thymine were prepared as references (**B-1-Me**, **B-2-Me** and **B-3-Me**), which are unable to form strong H-bond with **C-1**. Triple H-bonds are formed between each Bodipy antenna (**B-1**, **B-2** and **B-3**) and the C_{60} module (**C-1**). The photophysical properties of the H-bond assemblies and the reference non-hydrogen bond-forming mixtures were studied with steady state UV/vis absorption spectroscopy, fluorescence emission spectroscopy, electrochemical characterization, and nanosecond transient absorption spectroscopy. Singlet energy transfer from the Bodipy antenna to the C_{60} module was confirmed by fluorescence quenching studies. The intersystem crossing of the latter produce the triplet excited state. The nanosecond transient absorption spectroscopy shows that the triplet state is either localized on the C_{60} module (for assembly **B-1•C-1**), or on the styrylBodipy antenna (for assemblies **B-2•C-1** and **B-3•C-1**). Intra-assembly forward-backward ping-pong singlet/triplet energy transfer were proposed. In contrast to the H-bonding assemblies, slow triplet energy transfer was observed for the non-hydrogen bonding mixtures. As a proof of concept, these supramolecular assemblies were used as triplet photosensitizers for triplet-triplet annihilation upconversion.

1. Introduction

Triplet photosensitizers (PSs) have attracted much attention due to the applications in photocatalysis,[1–5] photodynamic therapy,[6–8] and more recently the triplet-triplet annihilation upconversion.[9–12] Conventional triplet PSs include the porphyrins, halogenated xanthane such as Rose Bengle and Methylene blue, and transition metal complexes such as Pt(II), Ru(II) or Ir(III) complexes, etc.[13–15] Recently halogonated Bodipys were developed as a new family of triplet PSs due to the feasible derivatized molecular structures, good photostability and strong absorption of visible light.[7,16]

There are a few challenges to be addressed in the molecular designing of new triplet PSs. First, most of the known triplet PSs contain heavy atoms to facilitate efficient intersystem crossing (ISC).[7,14,16] However, for some chromophores, it is difficult to introduce heavy atom into the molecular structure and the heavy atom effect may become non-efficient for chromophore with short S_1 state lifetime, or in bulky chromophores.[13b,14] On the other hand, heavy atom-free organic triplet photosensitizers are difficult to be '*designed*' because the ISC capability of such chromophore is almost unpredictable.[14] Second, the known triplet PSs are based on a integrated molecular structure motif, i.e. the visible light-harvesting and the ISC are implemented by the same chromophore, or by covalent bonded chromophores in a dyad/triad triplet PSs, for example the recently developed broadband visible light-absorbing organic triplet PSs.[7,14] This approach makes it synthetically demanding if a library of chromophores are to be screened for preparation of triplet PSs.[5,17-19] Therefore, new methods are desired for feasible preparation of organic triplet PSs.

Concerning this aspect, supramolecular assembly is in

particular interesting due to the advantage to fabricate molecular assemblies with different modules.[20,21] For example, the supramolecular photochemistry of the hydrogen bonded C_{60}-ferrocene dyad was studied.[22a] But the components show weak absorption of visible light, thus the assembly is unsuitable to be used as triplet PSs. Recently rotaxane with fluorescence-resonance-energy-transfer (FRET) was studied, but the fluorophore used in the rotaxane is unable to produce any triplet excited state upon photoexcitation.[22b]

In order to address the above challenges in the area of triplet PSs, herein we propose to use hydrogen bonded molecular assembly as a new approach for designing of organic triplet PSs.[23–25] This method is also useful for designing heavy atom-free triplet PSs. One of the hydrogen bonding modules is used as visible light-harvesting antenna and singlet energy donor, whereas the complementary H-bonding module was used as singlet energy acceptor and at the same time, the spin converter for triplet formation.[14] The disctance between the energy donor and acceptor can be controlled and singlet energy transfer is ensured. With this method, a wide variety of singlet energy donor can be feasibly screened because the H-bonded molecular assembly is easy to attain: simply mixing the H-bond donor and the H-bond acceptor in appropriate solvents, and the triplet formation upon photoexcitation can be feasibly evaluated by various spectroscopic methods. We confirmed this new molecular designing concept with preparation of H-bonded Bodipy/C_{60} assembly. Efficient and fast intra-assembly singlet and triplet energy transfer was observed, based on steady state and nanosecond transient absorption spectrocopy. In contrast, much slower intermolecular triplet state energy transfer was observed for the reference modules with which no H-bond can be formed. The application of the H-bond assemblies in singlet oxygen ($^1O_2$) photosensitizing and TTA upconversion was studied. This molecular designing method will be useful for study of organic triplet photosensitizers.

2 Results and Discussions

2.1 Molecular designing rational

A *N*-acetyl-1,6-diaminopyridine-Thymine based triple hydrogen bonding motif was used (Scheme 1–3). Thymine was connected to different Bodipy derivatives as visible light-harvesting H-bonding module, i.e. the singlet energy donor. The *N*-acetyl-1,6-diaminopyridine unit was connected to C_{60}, i.e. **C-1** (Scheme 1), as singlet energy acceptor and spin converter for triplet formation.[22a,26–29] Note the visible light-absorbing ability of the C_{60} is very weak,[30] but it is a good singlet energy acceptor because of the low S_1 state energy level (1.76 eV).[31–37]

Bodipy was selected as the visible light–harvesting antenna, due to the satisfactory photophysical properties, and the feasibly derivatizable molecular structures.[38–42] The Bodipy unit in **B-1** shows absorption at ca. 505 nm, whereas in **B-2** and **B-3** the styryl Bodipy unit shows absorption at 627 nm and 592 nm, respectively (Scheme 2).[43] H–bonded assemblies with different absorption wavelength can be feasibly prepared with **B-1**, **B-2** or **B-3** as visible light-harvesting H-bonding module, and with **C-1** as the singlet energy acceptor and the spin converter (Scheme 3). In order to study the effect of H-bonding on the photophysical processes, singlet energy donors **B-1-Me**, **B-2-Me** and **B-3-Me** (Scheme 2 and Scheme 3), which are unable to form H-bonds with **C-1**, were prepared. These reference compounds contain methyl group at the *N*-position of the thymine, as a result the H-bonding with **C-1** is substantially inhibited.[27–29] All the compounds were prepared with the routine synthetic methods and the compounds were obtained with moderate to satisfactory yields. The molecular structures were fully characterized with ^{1}H NMR, ^{13}C NMR, HR MS.

2.2. UV/vis absorption and fluorescence spectra

The UV/vis absorption spectra of the compounds were studied (Fig. 1). **C-1** gives the characteristic absorption of C_{60} unit, which is centered at 331 nm. For the singlet energy donor, i.e. the Bodipy derivatives, the absorption bands are located at 505 nm, 593 nm and 630 nm, respectively. The S_1 state energy level of C_{60} is 1.72 eV,[30,34] which is lower than the visible light-harvesting energy donors (**B-1**, **B-2** and **B-3**). The methylated visible light-harvesting compounds **B-1-Me**, **B-2-Me** and **B-3-Me** show similar absorption spectra as compared with the analogues without the methyl substitution on the *N* atom of thymine.

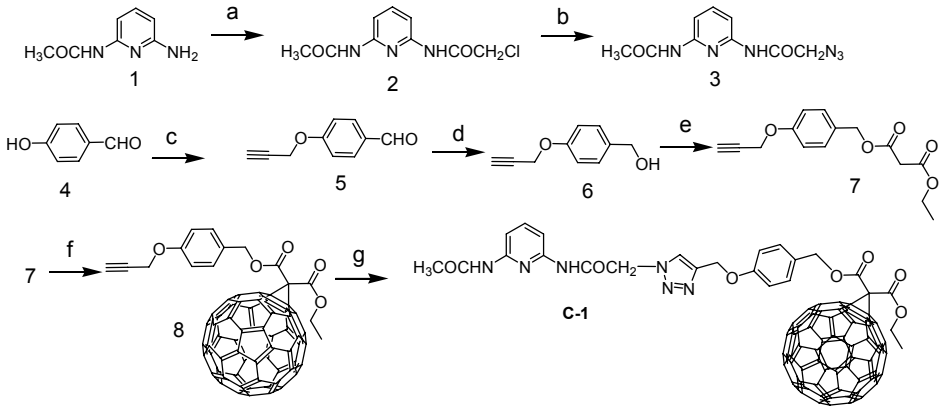

Scheme 1. Preparation of the hydrogen bonding C_{60} module **C-1**. (a) 2-Chloro-acetyl chloride, dry CH_2Cl_2, Ar, 25 °C, 2 h; (b) NaN_3, DMF, 70 °C, 5 hr; (c) 3-bromo-1-propyne, potassium carbonate, ethanol, 79 °C, 6 h; (d) $NaBH_4$, THF/CH_3OH, rt, 5 min; (e) methyl malonyl chloride, CH_2Cl_2, Ar, 25 °C, 12 h; (f) Iodine, C_{60}, DBU, toluene ,10 h, Ar, 25 °C; (g) Sodium ascorbate, $CuSO_4$, anhydrous $CHCl_3$/EtOH/water (12:1:1, v/v), rt, 12 h.

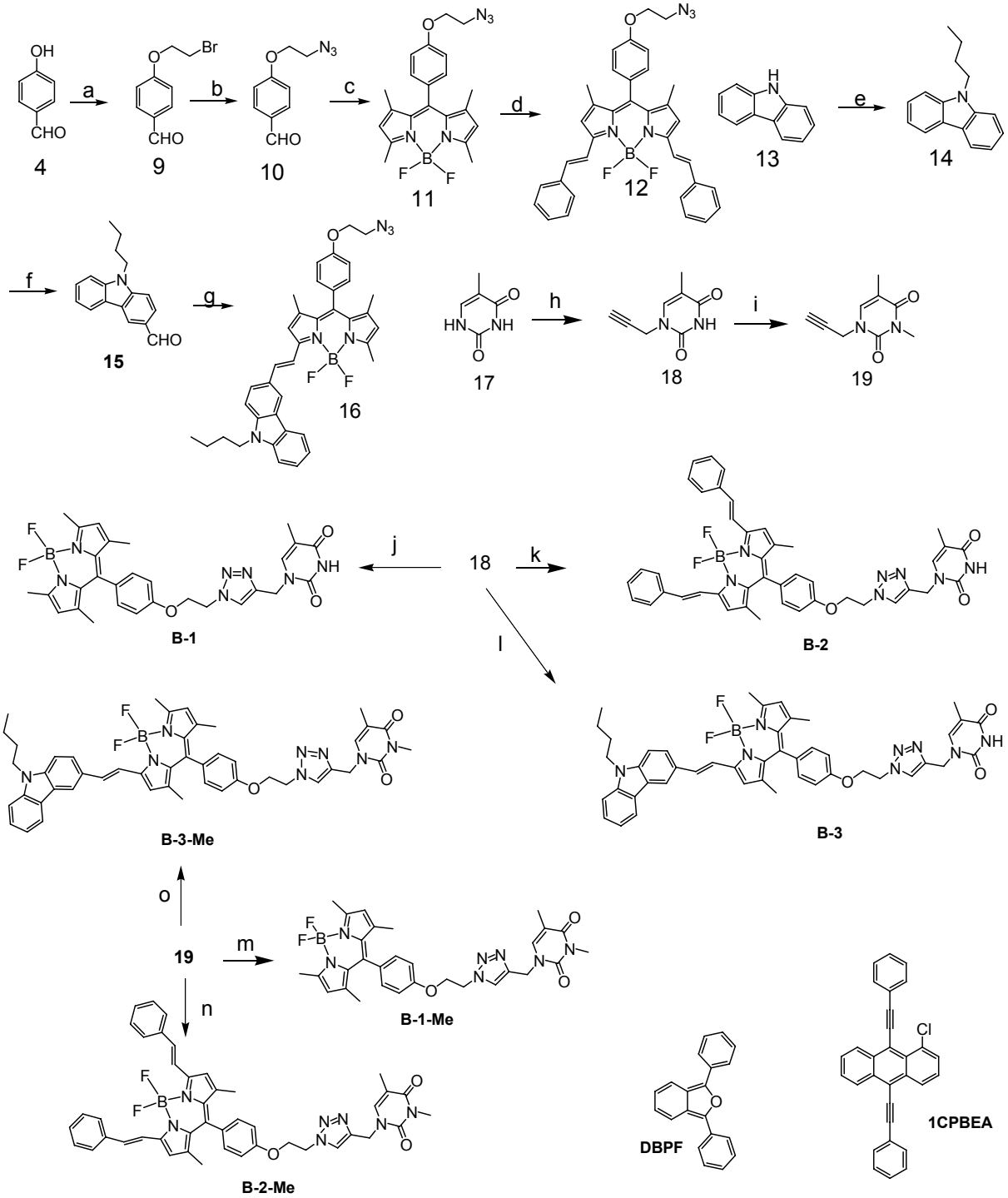

Scheme 2. Preparation of hydrogen bonding Bodipy modules **B-1**, **B-2**, **B-3** and the reference compounds which are unable to form tight hydrogen bonds with module **C-1**, i.e. **B-1-Me**, **B-2-Me** and **B-3-Me.** a) anhydrous K_2CO_3, 1,2-dibromoethane, dry ethanol, Ar, 70 °C; b) NaN_3, DMF, 100 °C, 10 h; c) 2, 4-dimethylpyrrole, TFA, anhydrous CH_2Cl_2, rt, 12 h; DDQ, $BF_3 \cdot Et_2O$, 12h; d) benzaldehyde, acetic acid, piperidine, microwave irradiation, 8 min; e) sodium hydride, *n*-Butyl bromide, DMF, rt, 2 h; f) DMF, $POCl_3$, rt, 3 h, 60 °C, 6 h; g) 9-butyl-9H-carbazole-3-carbaldehyde, acetic acid, piperidine, microwave irradiation, 5 min; h) propargyl bromide, K_2CO_3, DMF, rt, Ar, 10 h; i) NaH, Methyl iodide, rt, Ar, 12 h; j) 18, sodium ascorbate, $CuSO_4$, rt, Ar, 12 h; k) 18, sodium ascorbate, $CuSO_4$, rt, Ar, 12 h; l) 18, sodium ascorbate, $CuSO_4$, rt, Ar, 20 h; m) 19, sodium ascorbate, $CuSO_4$, rt, Ar, 12 h; n) 19, sodium ascorbate, $CuSO_4$, rt, Ar, 12 h; o) 19, sodium ascorbate, $CuSO_4$, rt, Ar, 24 h.

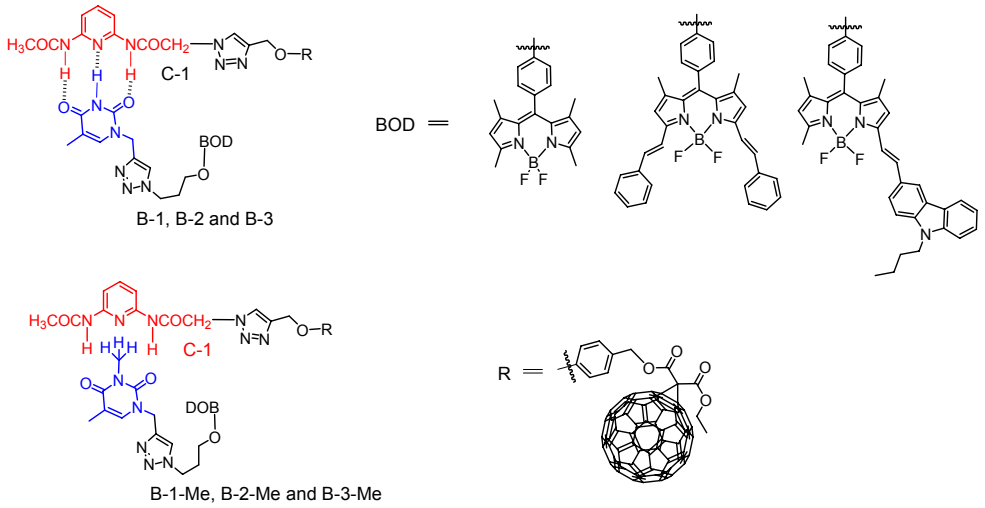

Scheme 3. Structure of the hydrogen-bonding assemblies (**C-1**/**B-1**, **B-2** and **B-3**, upper row); and the modules which are unable to form tight hydrogen bonds (**C-1**/**B-1-Me**, **B-2-Me** and **B-3-Me**. Lower row).

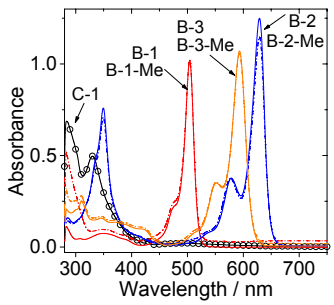

Fig. 1 UV/vis absorption spectra of **C-1**, **B-1**, **B-1-Me**, **B-2**, **B-2-Me**, **B-3** and **B-3-Me** (note the absorption of methylated Bodipy modules are identical to those are not methylated). $c = 1.0 \times 10^{-5}$ M in toluene. 20 °C.

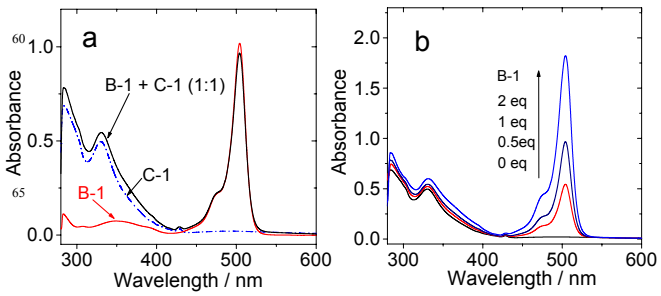

Fig. 2 UV/vis absorption spectra of (a) **B-1**, **C-1** and **C-1**/**B-1** (1/1); (b) **C-1** (1.0×10^{-5} M) with increasing the concentration of **B-1**. $c = 1.0 \times 10^{-5}$ M in toluene. 20 °C.

The UV/vis absorption of **C-1**/**B-1** in toluene, presumably H-bond formed, is superimposable to the sum of **B-1** and **C-1** (Fig. 2a). This result indicated that H-bonding does not induce any interaction between the Bodipy and C_{60} moieties at the ground state.[34] Similar results were observed for the mixture of **B-1-Me** and **C-1**, for which no H-bonding is expected (see ESI†, Fig. S45).[27] This conclusion was supported by titration of **C-1** with higher **B-1** concentration (2 eq. vs **C-1**. Fig. 2b).

In order to verify the H-bonding between the Bodipy visible light-harvesting unit and **C-1**, fluorescent titration of **B-1** with **C-1** was carried out (Fig. 3). The rational is that the fluorescence of **B-1** will be quenched by the energy transfer (such as through space energy transfer) to C_{60} given H-bond formed with **C-1**.[24,27,29,42b] **B-1** alone gives intense fluoresence at 517 nm (quantum yield Φ_F = 75.7%). Upon addition of **C-1** into the solution of **B-1**, however, the fluorescene intensity of **B-1** quenched substantially (Fig. 3a), and saturation was established with 12 eq. **C-1** added. The fluorescence intensity was reduced by 80 %. The hydrogen bonding process of **C-1** and **B-1** is a an equilibrium. In order for most of the **B-1** molecules to be H-bonded, i.e. in order to fully quench the fluorescence of **B-1**, excessive **C-1** has to be used. Interestingly, for **B-1-Me**, which is unable to form tight H-bond with **C-1** due to the methyl group on the *N* atom of thymine moiety, the fluorescence was quenched to much less extent, by 40 % with same amount of **C-1** was added (Fig. 3b). Therefore we propose tight H-bond formed for **C-1**/**B-1**, but not for **C-1**/**B-1-Me**.[27]

Similar fluorescence quenching profiles were observed for **B-2** and **B-3** (see ESI †, Fig. S51and S53). For example, the fluorescence emission wavelength of **B-3** is much longer than that of **B-1**. It should be pointed out that the S_1 state energy level of **B-3** (approxiamated as 2.04 eV) is still higher than that of **C-1** (1.76 eV), thus intra-assembly singlet energy transfer is ensured. For **B-3-Me**, no H-bond can be formed thus the quenching is to much less extent (see ESI †, Fig. S53b).

The fluorescence lifetimes of **B-1** (or **B-2**, or **B-3**) upon titration with **C-1** was measured (see ESI †, Table S68). The fluorescence lifetimes are nearly constant (3.5 ns – 3.4 ns) despite of the quenching of fluorescence intensity with increased **C-1** concentation. Thus we conclude that the fluorescence quenching is due to a mechanism similar to static quenching, not dynamic quenching,[44,45] upon formation of hygrogen bond. That is, the fluorescence of the H-bonded assembly is completely quenched, while the un-bonded Bodipy fluorophore will give the residual fluorescence.[44] In other words, the H-bonding assembly becomes non-fluorescent, and the residual fluorescence observed in the titration is due to the free Bodipy modules in the solution. In order to verify that the fluorescence quenching in the titration is due to H-bond

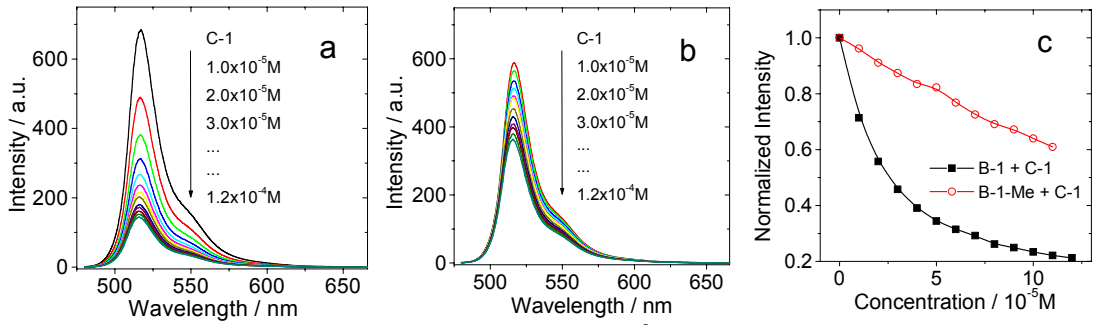

Fig. 3 Quenching of the fluorescence of (a) **B-1** and (b) **B-1-Me** by **C-1**. $c = 1.0 \times 10^{-5}$ M in toluene ($\lambda_{ex} = 475$ nm). (c) Emission intensity of **B-1** at 517 nm ($c = 1.0 \times 10^{-5}$ M in toluene), *versus* increasing concentration of [**C-1**] following excitation at 475 nm. 20 °C.

Table 1 Photophysical parameters of hydrogen bonding modules of bodipy and C_{60} [a]

	λ_{abs}	ε [b]	λ_{em}	Φ_F (%)	τ_F (ns)[f]
B-1	505	10.2	517	75.7[c]	3.5
B-1-Me	505	10.2	517	64.0[c]	3.6
B-2	630	12.4	642	73.5[d]	5.0
B-2-Me	630	11.5	642	65.4[d]	4.9
B-3	593	10.6	611	78.1[e]	3.7
B-3-Me	593	10.4	611	68.1[e]	3.9
C-1	331	5.1	–[g]	–[g]	–[g]

[a] In toluene (1.0×10^{-5} M). [b] Molar extinction coefficient at the absorption maxima. ε : 10^4 $M^{-1}cm^{-1}$. [c] With 2,6-diiodo-4,4-difluoro-1,3,5,7-tetramethyl-8-phenyl-4-bora-3a,4a-diaza-s-indacene as the standard (Φ = 71.2 % in acetonitrile). [d] With carbazolestyryl-bodipy as the standard (Φ = 0.72 % in toluene). [e] With carbazolestyryl-bodipy as the standard (Φ = 0.7 % in acetonitrile). [f] Fluorescence lifetimes. [g] Not determined.

mediated assembly, hexafluoroisoprapanol was added to disrupt the H-bonds. As a result, fluorescence recovery was observed (see ESI †, Fig. S54), which indicated that the fluorescence quenching was due to the formation of molecular assembly via H-bonding.

These studies with **B-1**, **B-2** and **B-3** as the visible light-harvesting chromophores to form molecular assembly with **C-1** demonstrates that the advantage of using H-bonding for preparation of intra-assembly energy transfer, that is, different combination can be easily accessed and screened for efficient intramolecular energy transfer and formation of triplet state.

The stability constants of the visible light-harvesting Bodipy and **C-1** were calculated based on the fluorescence titration experiments (Table 2).[46,47] The stability constants for the H-bond forming combinations show that the binding is tight. For the methylated Bodipy derivatives, however, the stability constants are 10-fold smaller.

2.3 Electrochemical studies and the free energy changes of the intramolecular electron transfer

In order to study the intra-assembly photoinduced electron transfer, the electrochemical properties of the Bodipy and the C_{60} modules were studied with Cyclic Voltammetry (Fig. 4).[34,48,49] For **B-1**, reversible reduction wave at −1.32 V was observed. A pseudo-reversible oxidation wave at +1.11 V was observed. Similar redox potentials were observed for **B-1-Me**. For **B-2**, the pseudo-reversible oxidation wave at +0.84 V was observed, which is shifted anodically as compared with **B-1**. For the carbazole-containing **B-3**, two reversible oxidation waves at +0.74 and +1.03 V were observed, which are different from **B-1** and **B-2**. The two reversible reduction waves of **B-3** and **B-3-Me** are due to the carbazole-styrylBodipy moiety, which is confirmed by study of a reference compound (see ESI †, Fig. S67). For the C_{60} module, i.e. **C-1**, two reversible reduction waves at −0.7 V and −1.08 V were observed (Fig. 5), as well as a pseudo-reversible reduction wave at −1.53 V. These reductions waves are attributed to the C_{60} moiety.

The plausible photoinduced intraassembly electron transfer between the Bodipy and the C_{60} module can be evaluated with the Gibbs free energy changes, which is calculated with the Rehm-Weller equation,[34,48,49]

$$\Delta G^0{}_{CS} = e[E_{OX} - E_{RED}] - E_{00} + \Delta G_S \quad \text{(Eq. 1)}$$

$$\Delta G_S = -\frac{e^2}{4\pi\varepsilon_S\varepsilon_0 R_{CC}} - \frac{e^2}{8\pi\varepsilon_0}\left(\frac{1}{R_D} + \frac{1}{R_A}\right)\left(\frac{1}{\varepsilon_{REF}} - \frac{1}{\varepsilon_S}\right) \quad \text{(Eq.2)}$$

Where ΔG_S is the static Coulombic energy, which is described by eq. 2. e is electronic charge, E_{OX} is half-wave potential for one-electron oxidation of the electron-donor unit, E_{RED} = half-

Table 2 The stability constants for the interaction of the Bodipy H-bonding module with H-bonding module **C-1**

	B-1	**B-1-Me**	**B-2**	**B-2-Me**	**B-3**	**B-3-Me**
K_{SV}/ $\mathbf{M^{-1}}$ [a]	4.08×10^4	3.02×10^3	3.67×10^4	1.22×10^3	5.14×10^4	5.43×10^3
K_b/ $\mathbf{M^{-1}}$ [b]	3.6×10^5	– [c]	1.38×10^6	– [c]	1.15×10^6	– [c]

[a] K_{SV} is linear Stern–Volmer quenching constant. [b] K_b represents the intrinsic binding constant of the compound with **C-1**. [c] Not applicable.

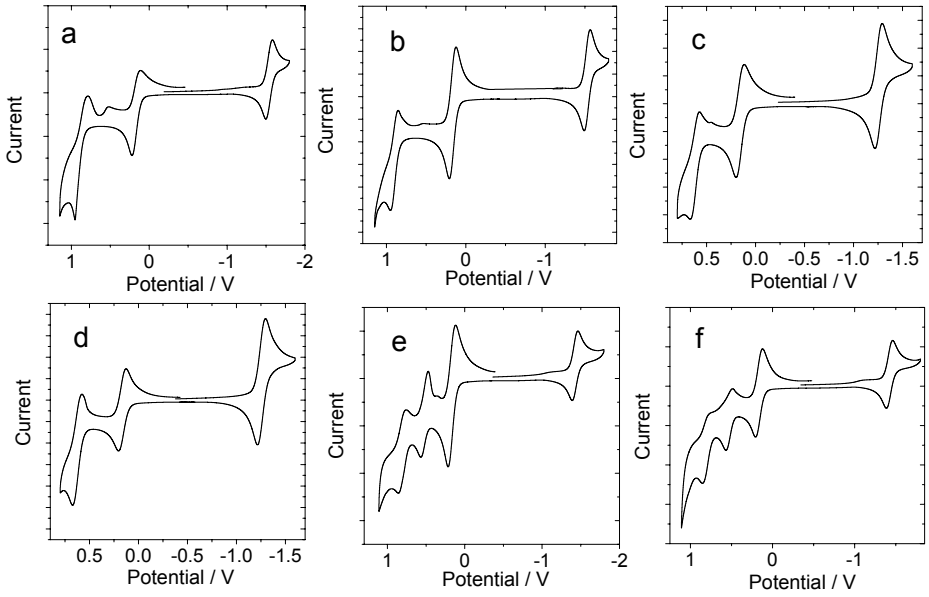

Fig. 4 Cyclic voltammogram of the bodipy H-bond modules. Ferrocene (Fc) was used as internal reference ($E_{1/2}$ = +0.38 V (Fc^+/Fc) vs. SCE). (a) **B-1**, (b) **B-1-Me**, (c) **B-2**, (d) **B-2-Me**, (e) **B-3**, (f) **B-3-Me**. In deaerated DCM solutions containing 0.5 mM photosensitizers alone, or with the ferrocene, 0.10 M Bu_4NPF_6 as supporting electrolyte, Ag/$AgNO_3$ reference electrode, Scan rates: 0.05 V/s.

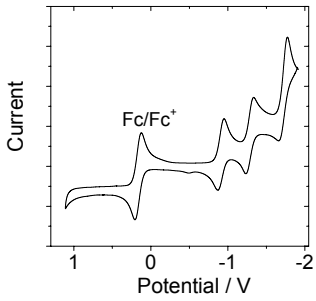

Fig. 5 Cyclic voltammogram of **C-1**. Ferrocene (Fc) was used as internal reference ($E_{1/2}$ = +0.38 V (Fc^+/Fc) vs. SCE). In deaerated DCM solutions containing 0.5 mM **C-1** alone, 0.10 M Bu_4NPF_6 as supporting electrolyte, Ag/$AgNO_3$ reference electrode, Scan rates: 0.05 V/s.

wave potential for one-electron reduction of the electron acceptor unit; E_{00} is energy level approximated with fluorescence emission (for the singlet excited state), ε_S = static dielectric constant of the solvent, R_{CC} = center-to-center separation distance between the electron donor (Bodipy module) and electron acceptor (**C-1** module), determined by DFT optimization of the geometry, R_{CC} (**B-1•C-1**) = 40.0 Å, R_{CC} (**B-2•C-2**) = 43.9 Å and R_{CC} (**B-1•C-1**) = 49.5 Å, R_D is the radius of the electron donor, R_A is the radius of the electron acceptor, ε_{REF} is the static dielectric constant of the solvent used for the electrochemical studies, ε_0 is permittivity of free space. The solvents used in the calculation of free energy of the electron transfer is toluene (ε_S = 2.4) and CH_2Cl_2 (ε_S = 8.93) The electrochemical data and the free energy changes of the photoinduced electron transfer in the H-bonding assemblies were summarized in Table 3. The results show that intra-assembly photo-induced electron transfer is thermodynamically prohibited. Therefore, the fluorescence quenching effect observed in the H-bonding titration (Fig. 3) is due to intra–assembly energy transfer, not electron transfer.

2.4 Nanosecond transient absorption spectroscopy: intra-assembly and intermolecular triplet state energy transfer

H-bonding formation between the Bodipy visible light-harvesting chromophores and the fullerene module **C-1** will induce singlet energy transfer from Bodipy to C_{60} part.[34,49] As a result, triplet excited state will be produced via the inherent ISC of C_{60}.[35–37] Thus nanosecond transient absorption spectroscopy was used to confirm the production of triplet state via the H-bonding mediated intra-assembly energy transfer.[22a] Indeed we observed the triplet state of **C-1** upon photoexcitation (no signal can be detected in aerated solution, see ESI †, Fig. S55).

First, **C-1** was titrated with **B-1** (Fig. 6). The mixed solution was photoexcited at 495 nm with nanosecond pulsed laser. The absorption of **C-1** at 495 nm is weak. Thus selective excitation of **B-1** in the mixture is possible. With increasing the concentration of **B-1**, the excited state absorption (ESA) of the C_{60} part at 715 nm was enhanced (indicated by the ΔO.D. values, which is proportional to the population of the transient species, Fig. 6f), indicated enhanced singlet energy transfer and finally the production of triplet state with increasing of **B-1** (Fig. 6d). The triplet state feature was confirmed by measurement of the transient in aerated solution (no signal was observed, see ESI†, Fig. S65 and S66). It should be pointed out that the triplet excited state is localized on the C_{60} moiety, not on the Bodipy moiety, because the ground state bleaching band at 505 nm (at which Bodipy unit gives steady state absorption) was not observed. This is in agreement with our previous studies of C_{60}-Bodipy dyads.[35] The triplet state lifetimes are in the range of 40.9 μs – 44.2 μs, which supports the localization of the triplet state on C_{60} moiety.[30] In comparison, excitation of **B-1** alone doesn't produce any triplet state (see ESI†, Fig. S62a), thus the cascade singlet energy transfer and ISC in the assembly **B-1•C-1**.

Table 3 Redox potentials of the H-bond modules and the of free-energy changes (ΔG_{ET}, PET) for the intramolecular electron transfer (with Bodipy unit as electron donor and the C_{60} unit as electron acceptor). Anodic and cathodic peak potential were presented. The potential values of the compounds are vs. SCE (saturated calomel electrode), with Fc as internal reference ($E_{1/2}$ (Fc^+/Fc) = +0.38 V) [a]

	E(ox) (V)	*E*(red) (V)	ΔG_{CS} (eV)
B-1	+1.11	−1.32	+0.21,[b] 1.17 [c]
B-1-Me	+1.12	−1.31	+0.25,[b] 1.33 [c]
B-2	+0.84	−1.04	+0.28,[b] 0.92 [c]
B-2-Me	+0.84	−1.04	+0.32,[b] 1.06 [c]
B-3	+0.74/+1.03	−1.21	+0.36,[b] 0.97 [c]
B-3-Me	+0.74/+1.03	−1.22	+0.40,[b] 1.14 [c]
C-1	– [d]	−0.70/−1.08/−1.53	– [e]

[a] Cyclic voltammetry in Ar saturated acetonitrile containing 0.10 M Bu_4NPF_6 supporting electrolyte; Counter electrode is Pt electrode; working electrode is glassy carbon electrode; Ag/$AgNO_3$ couple as the reference electrode. *c* [Ag^+] = 0.1 M. 0.5 mM dyad photosensitizers in DCM, 20 °C. Conditions: 0.5 mM dyad photosensitizers and 0.5 mM ferrocene in CH_2Cl_2, 293 K. [b] With reference **C-1** as electron acceptor, In CH_2Cl_2. [c] With reference **C-1** as electron acceptor, In toluene. [d] No reduction potential were observed, or no ΔG_{cs} values were calculated. [e] At r.t.

The quantum yields of the **C-1** and the **B-1•C-1** dygrodgen bonding assembly (1:1) were determined as 86.1 % and 67.5%, respectively, with the triplet energy transfer method, β-carotene as triplet energy acceptor, and $Ru(bpy)_3Cl_2$ as a reference (see Experimental section for details).[16b,16c]

The triplet state of **C-1** upon titration with **B-1-Me** was also studied (see ESI†, Fig. S56). Under this circumstance, no tight H-bonding is expected.[27] Intermolecular singlet energy transfer is unlikely for two compounds mechanically mixed in solution (the distant of the energy donor and the energy acceptor can be treated as infinite, well exceed the distant required for the Föster energy transfer). We did not observe any increase for the transient absorption of the T_1 state of C_{60} with increasing the concentration of **B-1-Me** (see ESI†, Fig. S56). Thus the intra-assembly singlet energy transfer was comfirmed by this reference compound.

Previously we demonstrated that for a Bodipy-C_{60} covalent dyad, intramolecular ping-pong energy transfer is possible, i.e. forward singlet energy transfer to the C_{60} unit, and the backward triplet energy transfer to the styrylBodipy visible light-harvesting chromophore.[36,37] Herein we studied this photophysical process with the H-bonding mediated supramolecular assemblies. To this end, **B-1** is not the proper candidate because the T_1 state energy level of C_{60} is lower that of the Bodipy unit in **B-1** therefore no backward triplet state energy transfer is expected, because the upward triplet energy transfer from C_{60} to the Bodipy unit in **B-1** is thermodynamically prohibited. Instead, we selected **B-3** for this kind of study because we have shown that the T_1 state of styrylBodipy-C_{60} dyad/triad is localized on the styrylBodipy moiety, not on the C_{60} unit. That is, styrylBodipy antenna is with lower T_1 state energy level than that of C_{60}.

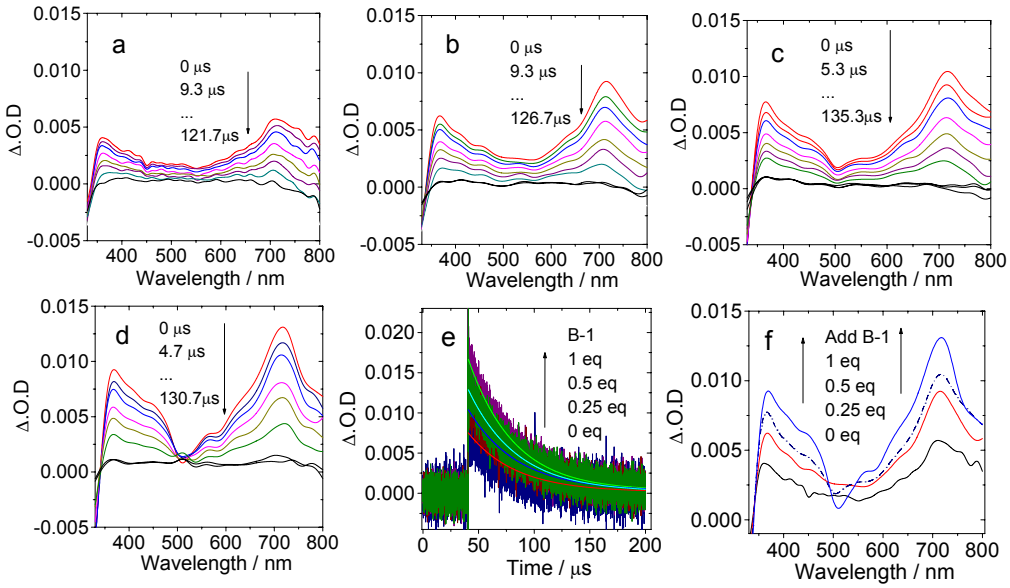

Fig. 6 Nanosecond transient absorption spectra of **C-1** with increasing amount of compound **B-1** added. The transient signal intensified with increasing **B-1** concentration at (a) 0 eq **B-1**; (b) 0.25 eq **B-1**; (c) 0.5 eq **B-1**; (d) 1 eq **B-1**; (e) Decay trace at 720 nm; (f) comparison of the transient absorption spectra at different **B-1** concentration with delay times at 0 μs. $c = 1.0 \times 10^{-5}$ M, In toluene after pulsed excitation at 495 nm under N_2. 20 °C.

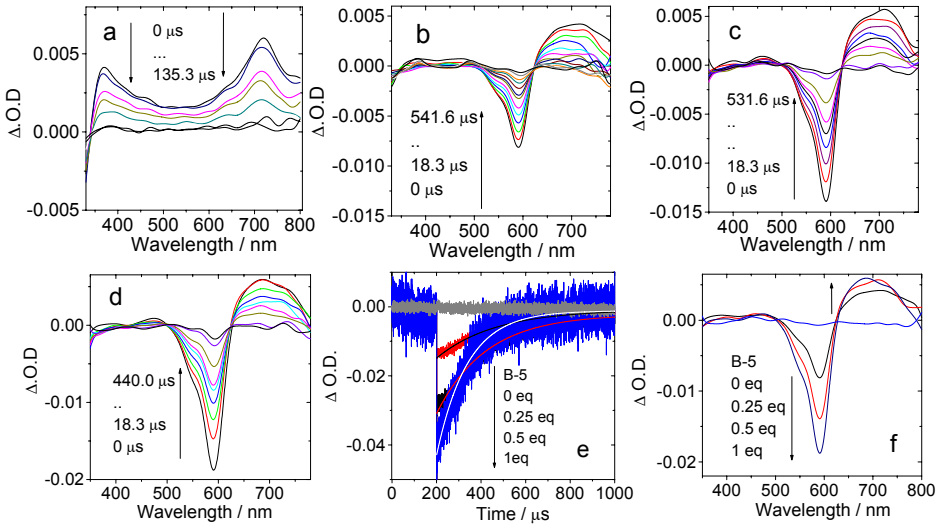

Fig. 7 Nanosecond transient absorption spectra of H-bonding module **C-1** upon titration with the complementary H-bonding module **B-3**. Transient absorption of **C-1** in the presence of (a) 0 eq **B-3**, (b) 0.25 eq **B-3**, (c) 0.5 eq **B-3**, (d) 1 eq **B-3**. Nanosecond transient absorption spectra of compound **C-1** with adding compound **B-3**. (e) Decay trace at 593 nm, (f) Transient spectra extracted from a-d at delay times of 0 μs. $c = 1.0 \times 10^{-5}$ M. In toluene after pulsed excitation at 590 nm under N_2. 20 °C.

For **B-3**, the excitation wavelength is 590 nm, at which the C_{60} unit shows weak absorption. With addition of **B-3** into the solution of **C-1**, bleaching band at 590 nm was observed, which can be assigned to the depletion of the ground state of carbazole styrylBodipy of **B-3** (Fig. 7b-d). ESA of the T_1 state ($T_1 \rightarrow T_n$ transitions) of styrylBodipy antenna was observed in the range of 600 nm – 750 nm.[35] Thus we propose there is ping-pong energy transfer in **B-3•C-1**. First, **B-3** was photoexcited with 590 nm laser, then intra-assembly singlet energy transfer from the carbazole StyrylBodipy to the H-bonded C_{60} moiety occurs. The ISC of C_{60} produces triplet excited state, followed by the backward triplet energy transfer from C_{60} to the carbazole StyrylBodipy module, as a result the ground state bleaching band and the ESA of the styrylBodipy part in **B-3** was observed.

With increasing of the **B-3** concentration, the ΔO.D. magnitude of **B-3** increased, indicated enhanced visible light-harvesting, the ping-pong singlet triplet energy transfer in the assembly and finally the production of the triplet excited state of the antenna (Fig. 7f). With 0.25 eq. to 1 eq. **B-3** was added, the triplet state lifetime decreased from 263.2 μs to 138.9 μs. The self-quenching constant is 4.6×10^5 M^{-1} s^{-1}. This quenching effect is due to the TTA process, which is significant for transient species with long triplet state lifetime. Similar fast intra-assembly TTET was observed for **B-2•C-1** (see ESI †, Fig. S58).

No strong H-bond should be formed with **B-3-Me**/**C-1**. The nanosecond transient absorption spectroscopy of **B-3-Me** in the presence of **C-1** was also studied (Fig. 8). Drastically different results were observed as compared with that of **B-3**/**C-1**. Bleaching band of the carbazole-styrylBodipy moiety was observed at 593 nm (Fig. 8b). Since C_{60} was excited at 425 nm, and excitation of the solution of **B-3-Me** alone did not produce any triplet excited state (see ESI †, Fig. S64a), the population of the T_1 state of the styrylBodipy moiety in **B-3-Me** is attributed to the *intermolecular* triplet energy transfer with C_{60} as the triplet energy donor.[50]

The evidence for this *intermolecular* energy transfer, rather than an *intra-assembly* fast energy transfer, is the biphase feature of the decay traces of the transient monitored at 630 nm (Fig. 8e and f), for which the first phase of increasing of the bleaching band at 593 nm is due to the intermolecular triplet energy transfer from C_{60} moiety to the styrylBodipy moiety in **B-3-Me**, which takes ca. 15 μs. This process is the relatively slow intermolecular TTET as compared to the fast intra-assembly TTET (Fig. 7e), for which the TTET is unable to be resolved with the transient absorption spectrometer (resolution spectrometer is 10 ns). The later recovery phase is due to the decay of T_1 state of the styrylBodipy moiety. The lack of formation of H-bonded molecular assembly for **B-3-Me**–**C-1** was confirmed by the ΔO.D. values of the transient absorption upon 425 nm and 590 nm photoexcitation (Fig. 8d). The ΔO.D. value of the transient upon excitation at 590 nm (where the styrylBodipy antenna gives strong absorption) is weaker than that with 425 nm excitation, and no slow increasing of the bleaching band was observed upon 590 nm photoexcitation. This result confirmed that there is no significant formation of H-bonding mediated molecular assembly.

For **B-2-Me**, such a slow evolvement of transient bleaching was also observed (see ESI †, Fig. S61). The triplet state energy transfer takes about 16 μs. This slow process is in stark contrast to that observed for the H-bonding assemblies of **B-2•C-1**, and **B-3•C-1**, for which there is no such slow increasing phase in the transient signal was observed. Thus the intra-assembly (in other words the intramolecular) triplet energy transfer is with rate constant $k_{TTET} > 10^8$ s^{-1} (the time-resolution of the spectrometer is 10 ns). This is an interesting result since for **C-1•B-2** or the **C-1•B-3** assembly, the distance between the C_{60} and the styrylBodipy part is ca. 5.0 nm, and the linker is with saturated bond, yet the triplet energy transfer is fast.[33,51] We propose the movement of the Bodipy module and the C_{60} module, thus intramolecular collision, makes the fast intra–assembly triplet state energy transfer occuring.

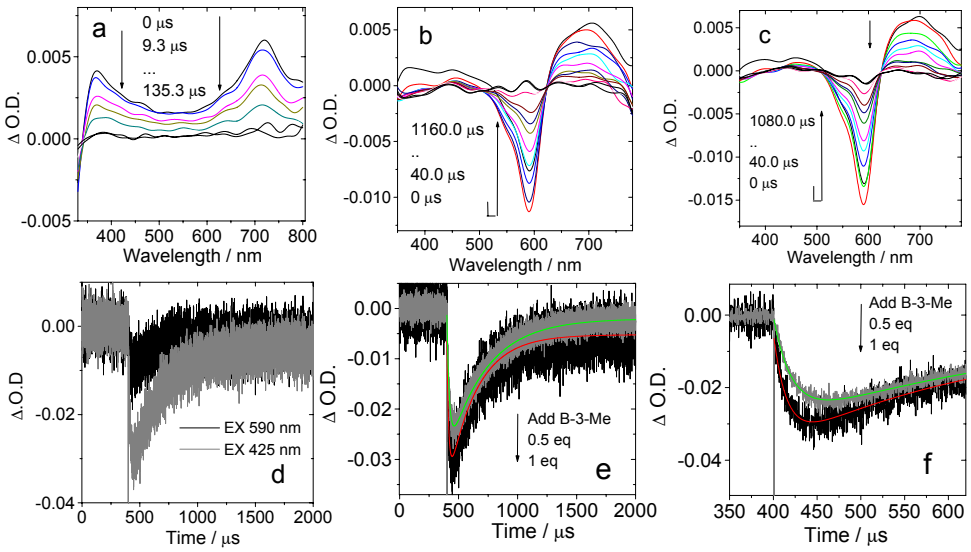

Fig. 8 Nanosecond transient absorption spectra of H-bonding module **C-1** upon titration with the non-preferred H-bonding module **B-3-Me** (no tight H-bond can be formed with **C-1**). Transient absorption spectra of **C-1** in the presence of (a) 0 eq **B-3-Me**, (b) 0.5 eq **B-3-Me** and (c) 1 eq **B-3-Me**. (d) Decay trace at 630 nm with **B-3-Me** added upon pulsed excitation at 425 nm (selectively excitation into the C_{60} moiety) and 590 nm (selectively excitation into the carbazole styrylBodipy moiety)。 (e) Decay trace at 630 nm with 0.5 eq. and 1eq. **B-3-Me** added. $c = 1.0 \times 10^{-5}$ M for **C-1** in toluene after pulsed excitation at 425 nm under N_2 (Note for sake of signal intensity the excitation is at 425 nm, instead of the 590 nm used in Fig. 7). (f) Magnification of the decay trace in (e). 20 °C.

Previously intra-assembly triplet energy transfer was observed for a hydrogen bonded C_{60} ferrocence dyad, from C_{60} to ferrocence ($k = 9.2 \times 10^5$ s^{-1}).[22a] Steroid-linked norbornadiene-carbazole dyad shows intramolecular triplet energy transfer with rate constant of 3.3×10^5 s^{-1} (from carbazole to norbornadiene moiety).[52] For the hydrogen bonded assembly **B-2•C-1** or **B-3•C-1**, the intramolecular triplet energy transfer from the C_{60} moiety to the styrylBodipy moiety is much faster ($k > 10^8$ s^{-1}). Triplet energy transfer is very often believed to be via Dexter electron exchange mechanism, which requires close contact of the energy donor and the energy acceptor. The triplet energy transfer will be negligible given the distance between the energy donor and acceptor exceed the sum of their van der Waals radii. We propose that the flexible chain in the assembly of **B-2•C-1** and **B-3•C-1** allow direct contact of the styrylBodipy and the C_{60} moiety in some foldamers, thus the triplet energy transfer is greatly accelerated. Previously hydrogen bonding porphyrin-Zinc porphyrin assemblies were studied, 50-80 times faster singlet-singlet energy transfer was observed for the assembly with flexible linker as compared with that of rigid linker, such as steroid.[53]

2.5 Molecular dynamics (MD) simulations: explanation of the fast intramolecular triplet energy transfer:

The possible conformation of complex including hydrogen acceptor and donor was explored by molecular dynamics (MD) simulations performed in aqueous solution (see ESI †).[53] It was found that a relative stable complex can be formed in less than 10 ns, indicating that the recognition of hydrogen donor and acceptor is rather feasible in aqueous solution. Note that three pairs of hydrogen bonds in the initial conformation are largely preserved in the compact conformation, although **B-3** prefers to assume an extended conformation in solution. Weak π-π interactions between partial **B-3** structure and fullerene motif of **C-1** molecules may further contribute the stability of such complex. These results indicate that fast intra-assembly TTET is possbile, which can be used for rationalization of the nanosecond transient absorption spectra of the H-bond assembly of (**B-3•C-1**).

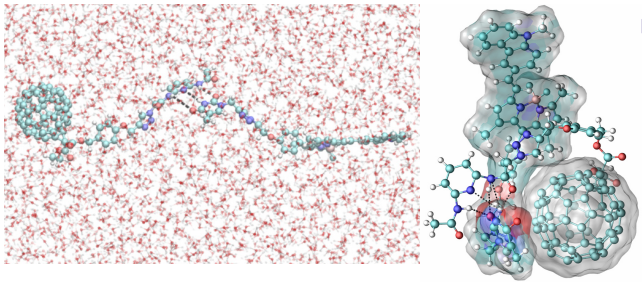

Fig. 9 Right: Conformations of **B-3•C-1** complex in aqueous solution taken from MD simulation at 6.9 ns, showing the hydrogen bonds (<3 Å as indicated using black dotted lines) between **B-3** and **C-1** motif. Left: the starting extended conformation used in MD simulations. The white surfaces represent the solvent (water molecules) accessible surface areas for **B-3** and fullerene motif of **C-1** structures.

2.6 Hydrogen-Bonded Bodipy/C_{60} assemblies as singlet oxygen ($^1O_2$) photosensitizer

The production of triplet excited state by the hydrogen-bonded C_{60}-Bodipy assemblies was also studied with the singlet oxygen ($^1O_2$) photosensitizing (Fig. 10). 1,3-diphenylbenzofuran (DPBF) was used as $^1O_2$ scavenger. The production of $^1O_2$ can be monitored by following the absorbance changes of DPBF at 414 nm.

For all the hydrogen bond formation assemblies, i.e. **B-1•C-1**, **B-2•C-1** and **B-3•C-1**, the $^1O_2$ photosensitizing ability is higher than the combinations that no tight hydrogen bond is

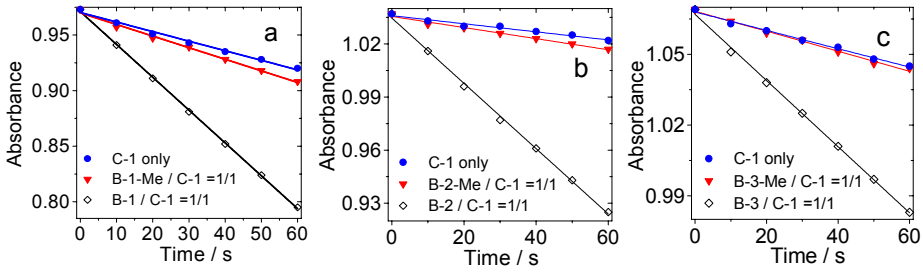

Fig. 10 Singlet oxygen ($^1O_2$) generation with photoexcitation of **C-1**, **B-1**, **B-1-Me**, **B-2**, **B-2-Me**, **B-3**, **B-3-Me** hydrogen bonded pairs are more efficient to produce $^1O_2$. Absorbance decrease of DPBF vs. photoirradiation time in the presence of photosensitizers: (a) λ_{ex} = 495 nm, 1.1 mW/m^2; (b) λ_{ex} = 630 nm, 1.3 mW/m^2; (c) λ_{ex} = 588 nm, 1.3 mW/m^2; c = 1.0 × 10^{-5} M in toluene. 20 °C.

able to form, i.e. **B-1-Me•C-1**, **B-2-Me•C-2**, and **B-3-Me•C-1**. These pairs show similar $^1O_2$ photosensitizing ability with that of **C-1** only. These results clearly demonstrated the effect of hydrogen bonding for intra-assembly singlet fenergy transfer.

2.7 Application in triplet-triplet annihilation upconversion

Up to now no supramolecular triplet photosensitizers were reported for TTA upconversion. The H-bonding assemblies were used as supramolecular triplet photosensitizers for TTA upconversion with 1-chloro-9,10-bisphenylethynylanthracene (1-CBPEA) as triplet acceptor/emitter. (Fig. 11. Note for **B-3** and **B-3-Me**, the fluorescence emission is with vibrational progression, i.e. there are two emission bands at 616 nm and 657 nm, respectively. Actually there should be no peak at 550 nm, it is due to the filter, because the transmittance is greatly reduced beyond 570 nm, thus the tailing of the emission band at give a fake 'peak' at 550 nm). For **B-3•C-1**, upconverted emission in the 450 – 550 nm region was observed with increasing of the **C-1** concentration (Fig. 11a). For **B-3-Me**, which is unable to form H-bonded molecular assembly, no TTA upconversion in the region of 450 nm – 550 nm was observed. Thus we confirm that the triplet state production with **B-3•C-1** upon photoexcitation is sufficient for TTA upconversion. For the **B-3-Me**/**C-1**, mixture, however, no upconversion was observed due to the lack of H-bonding. To the best of our knowledge, this is the first time that a supramolecular triplet photosensitizer was used for TTA upconversion. This result opens a new avenue for the studies on the TTA upconversion.

In order to prove that the production of the triplet excited state, as well as the TTA upconversion, are based on the formation of the H-bonded molecular assembly, hexafluoroisopropanol (HFIP) was added to disrupt the H-bond (Fig. 11c). As a result, the TTA UC intensity decreased, at the same time, the fluorescence of the antenna was enhanced. These changes are in agreement that the H-bond was disrupted. Note the upconversion is weak, but this proof-of-concept approach will be useful for designing supramolecular triplet photosensitizers and for the application of the compounds. For **B-3-Me**, no such enhancement of the fluorescence of antenna was observed in the presence of HFIP (Fig. 11d).

3. Conclusion

In summary, hydrogen-bond-mediated supramolecular molecular assemblies of Bodipy and C_{60} modules were prepared as supramolecular triplet photosensitizers. Intra-assembly singlet and triplet state energy transfer were observed. The molecular assemblies were used as supramolecular triplet photosensitizers for triplet-triplet annihilation upconversion. Three different thymine-containing visible light-harvesting Bodipy derivatives (**B-1**, **B-2** and **B-3**, which show absorption at 505 nm, 630 nm and 593 nm,

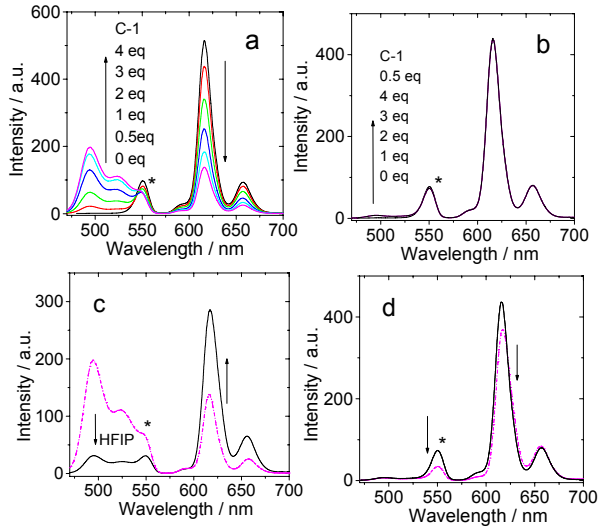

Fig. 11 TTA upconversions of **C-1** with H-bonding modules of **B-3** and **B-3-Me**. **1-CBPEA** was used as triplet acceptor. The emission of (a) **B-3** and **1-CBPEA** with increasing **C-1** added; (b) **B-3-Me** and **1-CBPEA** with increasing **C-1** added; (c) 0 μL and 100 μL of hexafluoroisopropanol (HFIP) added in the mixed solution of **B-3**, **1-CBPEA** and 4 eq **C-1** to disrupt the H-bonding; (d) 0 μL and 100 μL of HFIP added in the mixed solution of **B-3-Me**, **1-CBPEA** and 4 eq **C-1**. Excited with 589 nm laser (4.4 mW, power density is 60 mW cm^{-2}) and a band-pass filter (470 nm – 570 nm) was used to suppress the scattered laser. The asterisks indicated the residual of the emission of the antenna. c[Photosensitizers] = 1.0 × 10^{-5} M. c [**1-CBPEA**] = 1.2 × 10^{-4} M in deaerated toluene. 20 °C.

respectively) were used as one of the H-bonding modules, whereas 1,6-diaminopyridine appended C_{60} was used as the complementary hydrogen bonding module (**C-1**). Visible light-harvesting antenna with methylated thymine were prepared as reference compounds (**B-1-Me**, **B-2-Me** and **B-3-Me**), which are unable to form strong H-bond with **C-1**. Triple H-bond are formed between each Bodipy module (**B-1**, **B-2** and **B-3**, visible

light-harvesting antenna) and the bonding module (**C-1**). The photophysical properties of the assemblies were studied with steady state UV/vis absorption spectroscopy, fluorescence emission spectroscopy, electrochemical characterization, and nanosecond transient absorption spectroscopies. Singlet energy transfer from the Bodipy antenna to the C_{60} module was confirmed by the fluorescence quenching studies. The methylated modules are unable to firm tight H-bond with **C-1**, fluorescence quenching was observed as less extent. The nanosecond transient absorption spectroscopy show that the triplet state is either localized on the C_{60} module (assembly **B-1•C-1**), or on the Bodipy antenna (for assemblies **B-2•C-1** and **B-3•C-1**). For assembly **B-1•C-1**, the photophysical processes are either intra-assembly singlet energy transfer from the antenna to the C_{60} module, then the intersystem crossing of the latter produce the triplet excited state. The triplet state is localized on the C_{60} part in assembly **B-1•C-1**. For **B-2•C-1** and **B-3•C-1**, intra-assembly ping-pong singlet/transfer energy transfer were proposed, as a result the triplet state is confined on the styrylBodipy part in **B-2•C-1** and **B-3•C-1.** No significant triplet state production was observed for the reference mixture of **B-1-Me/C-1**, **B-2-Me/C-1** and **B-3-Me/C-1**, for which no tight H-bonds were formed. These supramolecular assemblies were used as triplet photosensitizers for triplet-triplet annihilation upconversion. These studies may offer a new approach for designing of organic triplet photosensitizers.

4. Experimental section

4.1 Materials

UV/vis absorption spectra were measured with an Agilent 8453 spectrophotometer. Fluorescence spectra were recorded on a Shimadzu RF-5301PC spectrofluorometer. Luminescence lifetimes were measured on a OB920 luminescence lifetime spectrometer (Edinburgh Instruments, UK).

4.2 Synthesis

Synthesis of C-1. To the solution of **3** (0.04 mmol, 10 mg) in a mixed solvent $CHCl_3$/EtOH/water (12:1:1, v/v, 28 mL), **8** (0.043 mmol, 42.7 mg), sodium ascorbate (0.0237 mmol, 4.7 mg) and $CuSO_4$ (0.0118 mmol, 2.9 mg) were added successively. The mixture was stirred at RT for 12 h. Then water was added, and the mixture was extracted with CH_2Cl_2. The organic phase was dried over Na_2SO_4. The solvent was evaporated under reduced pressure. The crude product was purified by column chromatography (silica gel, CH_2Cl_2/CH_3OH, 50:1, v/v) to afford gray solid. Yield: 26.5 mg (50.2%). ^{1}H NMR (500 MHz, DMSO-d_6): 10.59 (s, 1H), 10.13 (s, 1H), 8.24 (s, 1H), 7.76–7.65 (m, 3H), 7.49 (d, 2H, J = 8.3 Hz), 7.11 (d, 2H, J =8.3 Hz), 5.50–5.46 (m, 4H), 5.17 (s, 2H), 4.50–4.44 (m, 2H), 2.12 (s, 3H), 1.29 (t, 3H, J =7.0 Hz). ^{13}C NMR (100 MHz, DMSO-d_6): 162.5, 144.2, 144.1, 144.0, 143.8, 143.7, 143.2, 140.0, 138.4, 137.7, 131.1, 114.5, 71.1, 60.7, 52.1, 30.7, 23.9, 13.9. HRMS: m/z calcd for $[C_{75}H_{14}O_5]^+$: 994.0841; found: 994.0844.

Synthesis of B-1. To the solution of **11** (0.18 mmol, 75 mg) in $CHCl_3$/EtOH/water (12:1:1, v/v, 28 mL), **18** (0.18 mmol, 30 mg), sodium ascorbate (0.0237 mmol, 4.7 mg) and $CuSO_4$ (0.0118 mmol, 2.9 mg) were added and the mixture was stirred at RT for 12 h. In a typical workup, water was added and the mixture was extracted with CH_2Cl_2. The organic phase was dried over sodium sulfate. After removal of the solvent, the product was purified by column chromatography (silica gel, CH_2Cl_2/CH_3OH, 25:1, v/v) to afford orange solid. Yield: 33.6 mg (32.6%). ^{1}H NMR (500 MHz, DMSO-d_6): 11.3 (s, 1H), 8.18 (s, 1H), 7.64 (s, 1H), 7.26 (d, 2H, J = 8.4 Hz), 7.09 (d, 2H, J = 8.5 Hz), 6.17 (s, 2H), 4.91 (s, 2H), 4.79 (t, 2H, J = 4.7 Hz), 4.46 (d, 2H, J = 4.6 Hz), 2.24 (s, 6H), 1.74 (s, 3H), 1.36 (s, 6H). ^{13}C NMR (100 MHz, $CDCl_3$): 163.8, 155.5, 150.6, 140.2, 128.2, 121.2, 114.9, 111.2, 66.3, 49.9, 42.9, 29.7, 14.6, 12.3. HRMS (MALDI): m/z calcd for $[C_{29}H_{30}N_7O_3F_2B]^+$: 573.2741; found: 573.2504.

Synthesis of B-1-Me. To the solution of **11** (0.15 mmol, 65 mg) in $CHCl_3$/EtOH/water (12:1:1, v/v, 14 mL), **19** (0.15 mmol, 26 mg), sodium ascorbate (0.0237 mmol, 4.7 mg) and $CuSO_4$ (0.0118 mmol, 2.9 mg) was added and the mixture was stirred at RT for 12 h. After the typical workup, the crude product was purified by column chromatography (silica gel, CH_2Cl_2/CH_3OH, 40:1, v/v) to afford orange solid. Yield: 35.6 mg (40.2%). ^{1}H NMR (500 MHz, $CDCl_3$): 8.00 (s, 1H), 7.41 (s, 1H), 7.20 (d, 2H, J = 6.5 Hz), 6.99 (d, 2H, J = 8.1 Hz), 5.98 (s, 2H), 5.03 (s, 2H), 4.82 (s, 2H), 4.43 (s, 2H), 3.33 (s, 3H), 2.54 (s, 6H), 1.93 (s, 3H), 1.39 (s, 6H). ^{13}C NMR (100 MHz, $CDCl_3$): 164.1, 158.8, 155.6, 151.8, 140.8, 131.9, 128.5, 121.4, 115.3, 110.5, 66.2, 50.4, 44.1, 28.1, 13.2. HRMS (MALDI): m/z calcd for $[C_{30}H_{32}N_7O_3F_2B]^+$: 587.2628; found: 587.2614.

Synthesis of B-2. To the solution of **12** (0.07 mmol, 40 mg) in $CHCl_3$/EtOH/water (12:1:1, v/v, 14 mL), **18** (0.07 mmol, 11.2 mg), sodium ascorbate (0.047 mmol, 9.4 mg) and $CuSO_4$ (0.0236 mmol, 5.8 mg) were added and the mixture was stirred at RT for 12 h. After the workup, the crude product was purified by column chromatography (silica gel, CH_2Cl_2/CH_3OH, 25:1, v/v) to afford blue solid. Yield: 33 mg (62.9%). ^{1}H NMR (500 MHz, $CDCl_3$): 8.64 (s, 1H), 7.94 (s, 1H), 7.75-7.84 (m, 6H), 7.41-7.26 (m, 11H), 7.00 (s, 2H), 6.64 (s, 2H), 4.96 (s, 2H), 4.80 (s, 2H), 4.41 (s, 2H), 1.88 (s, 3H), 1.46 (s, 6H). ^{13}C NMR (100 MHz, $CDCl_3$): 169.3 163.5, 157.4, 156.0, 147.8, 145.4, 143.6, 141.2, 138.6, 134.9, 132.4, 124.1, 122.7, 120.3, 115.7, 71.5, 54.9, 48.0, 34.7, 19.7,17.0. HRMS (MALDI): m/z calcd for $[C_{43}H_{38}N_7O_3F_2B]^+$: 749.3097; found: 749.3092.

Synthesis of B-2-Me. To the solution of **12** (0.05 mmol, 28 mg) in $CHCl_3$/EtOH/water (12:1:1, v/v, 14 mL), **19** (0.05 mmol, 8.5 mg), sodium ascorbate (0.047 mmol, 9.4 mg) and $CuSO_4$ (0.0236 mmol, 5.8 mg) were added and the mixture was stirred at RT for 12 h. After the workup, the crude product was purified by column chromatography (silica gel, CH_2Cl_2/CH_3OH, 40:1, v/v) to afford a blue solid. Yield: 33 mg (68.1%). ^{1}H NMR (400 MHz, $CDCl_3$): 7.91 (s, 1H), 7.77–7.63 (m, 6H), 7.39–7.68 (m, 13H), 7.64 (s, 2H), 6.64 (s, 2H), 5.00 (s, 2H), 4.77 (s, 2H), 4.40 (s, 2H), 3.34 (s, 3H), 1.93 (s, 3H), 1.46 (s, 6H). ^{13}C NMR (100 MHz, $CDCl_3$): 164.1, 158.5, 152.8, 152.0, 151.7, 148.0, 142.2, 138.7, 137.7,136.4, 133.8, 130.1, 129.0, 127.7, 125.0, 119.4, 118.0, 115.2, 110.4, 66.4, 50.0, 44.1, 28.1, 15.1,13.2. HRMS (MALDI): m/z calcd for $[C_{44}H_{40}N_7O_3F_2B]^+$: 763.3254; found: 763.3294.

Synthesis of B-3. To the solution of **16** (0.055 mmol, 35 mg) in $CHCl_3$/EtOH/water (12:1:1, v/v, 14 mL), **18** (0.05 mmol, 8.2 mg), sodium ascorbate (0.047 mmol, 9.4 mg) and $CuSO_4$ (0.0236 mmol, 5.8 mg) were added and the mixture was stirred at RT for 24 h. After the workup, the crude product was purified by column chromatography (silica gel, CH_2Cl_2/CH_3OH, 25:1, v/v) to afford a blue solid. Yield: 22.3 mg (50.2%). ^{1}H NMR (400 MHz,

$CDCl_3$): 8.99 (s, 1H), 8.28 (s, 1H), 8.17 (d, 2H, J = 7.6 Hz), 7.79–7.69 (m, 2H), 7.50–7.38 (m, 6H), 7.24–7.22 (m, 3H), 7.00 (s, 2H), 6.66 (s, 1H), 5.99 (s, 1H), 5.00 (s, 2H), 4.81 (s, 2H), 4.41 (s, 3H), 4.31 (t, 2H, J = 6.7 Hz), 2.62 (s, 3H), 1.88 (s, 3H), 1.44–1.40 (m, 8H), 0.96 (t, 3H, J = 6.7 Hz). ^{13}C NMR (100 MHz, $CDCl_3$): 164.4, 154.1, 151.2, 141.6, 140.8, 138.2, 133.3, 130.0, 123.4,120.8, 119.5, 117.6, 116.2, 115.1, 111.3, 109.2, 66.1, 43.1, 31.1, 30.1, 20.6,13.9, 12.3. HRMS (MALDI): m/z calcd for $[C_{46}H_{45}N_8O_3F_2B]^+$: 806.3676; found: 806.3685.

Synthesis of B-3-Me. To the solution of **16** (0.04 mmol, 25.6 mg) in a mixture of $CHCl_3$/EtOH/water (14 mL, 12:1:1, v/v), **19** (0.04 mmol, 7.1 mg), sodium ascorbate (0.047 mmol, 9.4 mg), $CuSO_4$ (0.0236 mmol, 5.8 mg) were added and the mixture was stirred at RT for 24 h. After the typical workup, the crude product was purified by column chromatography (silica gel, CH_2Cl_2/CH_3OH, 40:1, v/v) to afford a blue solid. Yield: 19.6 mg (59.7%). ^{1}H NMR (400 MHz, $CDCl_3$): 8.28 (s, 1H), 8.17 (d, 2H, J = 9.5 Hz), 7.78–7.69 (m, 2H), 7.50–7.38 (m, 5H), 7.25–7.22 (m, 4H), 7.00 (d, 2H, J = 7.4 Hz), 6.67 (s, 1H), 5.99 (s, 1H), 5.02 (s, 2H), 4.80 (s, 2H), 4.42 (s, 2H), 4.31 (t, 2H, J = 7.5 Hz), 3.34 (s, 3H), 2.62 (s, 3H), 1.93 (s, 3H), 1.47–1.38 (m, 8H), 0.96 (t, 3H, J = 6.4 Hz). ^{13}C NMR (100 MHz, $CDCl_3$): 164.1, 158.1, 154.3, 152.0, 143.0, 141.1, 138.3, 133.4, 128.8, 125.8, 123.5, 119.5, 117.6, 114.5, 110.5, 109.5, 66.2, 43.2, 29.5, 28.1, 20.92, 14.1,12.9. HRMS (MALDI): m/z calcd for $[C_{47}H_{47}N_8O_3F_2B]^+$: 820.3832; found: 820.3850.

4.3 Cyclic voltammetry

Cyclic voltammetry was performed using a CHI610D Electrochemical workstation (Shanghai, China). Cyclic voltammograms were recorded at scan rates of 0.05 V/s. The electrolytic cell used was a three electrodes cell. Electrochemical measurements were performed at RT using 0.1 M tetrabutylammonium hexafluorophosphate (TBAP) as supporting electrolyte, after purging with N_2. The working electrode was a glassy carbon electrode, and the counter electrode was platinum electrode. A nonaqueous Ag/ $AgNO_3$ (0.1 M in acetonitrile) reference electrode was contained in a separate compartment connected to the solution via semipermeable membrane. DCM was used as the solvent. Ferrocene was added as the internal references.

4.4 Nanosecond transient absorption spectra

The spectra were measured on LP920 laser flash photolysis spectrometer (Edinburgh Instruments, U.K.). The lifetime (by monitoring the decay trace) were calculated with the LP900 software. All before measurement and the gas flow is kept during the measurement. The samples were excited with a nanosecond pulsed laser (OpoletteTM 355II+UV nanosecond pulsed laser, typical pulse length: 7 ns. Pulse repetition: 20 Hz. Peak OPO energy: 4 mJ. The wavelength is tunable in the range of 410–2200 nm. OPOTEK, USA) and the transient signals were recorded on a Tektronix TDS 3012B oscilloscope.

The quantum yield of the triplet formation (Φ_T) was determined with the sensitizing method, which was described in detail previously.[16b,16c,54] The method is based on the using of a triplet energy acceptor (β-carotene), and a standard compound ($Ru(bpy)_3Cl_2$, bpy = 2,2′-bipyridine , Φ_T = 1). With optically matched solution of the reference, or the **C-1• B-1** hydrogen bonding assebly, and upon excitation at the same wavelength, the Δ O.D. value, and the triplet-triplet-energy-transfer to β-carotene (K_{TTET}, monitored at the $T_1 \rightarrow T_n$ absorption of at 515 nm), and the decay of the triplet energy donor in the absence of β-carotene (k_0) were used for calculation of the Φ_T values.

4.5 Computational simulations of B-1 and C-1 complex

Force filed parameters of B-1 and C-1 structures. The structures of **B-1** and **C-1** motif without fullerene were first energy minimized using density functional theory at B3LYP/6-31G* level. Frequency analyses were performed on the optimized structures in order to obtain the Hessian matrix, from which the corresponding force constants for all the bonds were calculated, as well as the equilibrium bond lengths. The electrostatic potential was calculated based on the same theory using Mulliken population analysis. The restrained electrostatic potential (RESP) method was used to fit the electrostatic potential to obtain the atomic partial charges.[55] All quantum chemical calculations were carried out with the Gaussian 09 software package.[56] The plug-in of PARATOOL in VMD was used to derive the corresponding force constants.[57] For the fullerene motif of **C-1**, the partial charges for all carbon atoms were set to zero, as indicated in previous molecular dynamics simulations of fullerene derivatives.[58,59] The force constants of CHARMM force field parameters[60] were applied for the bonded and non-bonded interactions within the fullerene motif of **C-1**.

Molecular dynamics simulations. The starting complex of **B-1** and **C-1** is extended, with three pairs of hydrogen bonds between **B-1** and **C-1**. This initial structure was solvated in a TIP3P water box (85 Å × 55 Å × 48 Å), resulting a system containing 6970 water molecules. The whole system was first minimized with **B-1•C-1** complex fixed for 5000 steps to remove unfavorable van der Waals contacts between solvent and solute molecules. Then the system was heated to the room temperature of 300 K gradually with **B-1•C-1** complex constrained with harmonic restraints. After a 50-ps equilibration at the desired temperature, the whole system was simulated for another 30 ns without restraints under the *NPT* ensemble (constant number of atoms, pressure and temperature). The temperature was maintained at 310 K using Langevin dynamics, and the pressure was kept at 1 atm using Langevin piston method. An integration time step of 2 fs was used. The long-range electrostatic interactions were treated using PME method. Trajectory was saved every 500 steps (1 ps). A hydrogen bond is formed if the donor atoms (H atom) within 3 Å of the acceptor atoms (N or O atoms). All molecular dynamics simulations were performed using NAMD 2.9 software.[61] The non-bonded interaction parameters were taken from CHARMM 27 force filed parameters.[60]

Acknowledgement

We thank the NSFC (21273028, 21473020 and 21421005), the Royal Society (UK) and NSFC (21011130154), Program for Changjiang Scholars and Innovative Research Team in University [IRT_13R06], State Key Laboratory of Fine Chemicals (KF1203), the Fundamental Research Funds for the Central Universities (DUT14ZD226) and Dalian University of

Technology (DUT2013TB07) for financial support.

Notes and references

[a] State Key Laboratory of Fine Chemicals E-208, West Campus, Dalian University of Technology, Dalian 116024 (P. R. China) Fax: (+) 86 411 8498 6236. E-mail: zhaojzh@dlut.edu.cn
Web: http://finechem2.dlut.edu.cn/photochem

[b] School of Chemistry, Dalian University of Technology, Dalian 116024 (P. R. China)

[c] Department of Engineering Physics, Faculty of Engineering, Ankara University, 06100 Beşevler, Ankara (Turkey)

[d] Department of Chemistry, Faculty of Science, Ankara University, 06100 Beşevler, Ankara (Turkey)

† Electronic Supplementary Information (ESI) available: synthesis and structure characterization data, UV/Vis absorption and emission spectra. See DOI: 10.1039/b000000x/.

1 J. Xuan and W. Xiao, *Angew. Chem. Int. Ed.*, 2012, **51**, 6828–6838.
2 D. P. Hari and B. König, *Angew. Chem. Int. Ed.*, 2013, **52**, 4734–4743.
3 J. M. R. Narayanama and C. R. J. Stephenson, *Chem. Soc. Rev.*, 2011, **40**, 102–113.
4 L. Shi and W. Xia, *Chem. Soc. Rev.*, 2012, **41**, 7687–7697.
5 D. Ravelli, M. Fagnoni and A. Albini, *Chem. Soc. Rev.*, 2013, **42**, 97–113.
6 Y. Cakmak, S. Kolemen, S. Duman, Y. Dede, Y. Dolen, B.Kilic, Z. Kostereli, L. T. Yildirim, A. L. Dogan, D. Guc and E. U. Akkaya, *Angew. Chem. Int. Ed.*, 2011, **50**, 11937–11941.
7. (*a*) A. Kamkaew, S. H. Lim, H. B. Lee, L. V. Kiew, L. Y. Chung and K. Burgess, *Chem. Soc. Rev.*, 2013, **42**, 77–88; (*b*) O. J. Stacey and S. J. A. Pope. *RSC Adv.*, 2013, **3**, 25550–25564; (*c*) F. Schmitt, J. Freudenreich, N. P. E. Barry, L. Juillerat-Jeanneret, G. Süss-Fink, and B. Therrien, *J. Am. Chem. Soc.*, 2012, **134**, 754–757; (*d*) A. Gorman, J. Killoran, C. O'Shea, T. Kenna, W. Gallagher and D. O'Shea , *J. Am. Chem. Soc.*, 2004, **126**, 10619–10631.
8 A. M. Bugaj, *Photochem. Photobiol. Sci.*, 2011, **10**, 1097–1109.
9 Y. C. Simon and C. Weder, *J. Mater. Chem.*, 2012, **22**, 20817–20830.
10 T. N. Singh-Rachford and F. N. Castellano, *Coord. Chem. Rev.*, 2010, **254**, 2560–2573.
11 J. Zhao, S. Ji and H. Guo, *RSC Adv.*, 2011, **1**, 937–950.
12 P. Ceroni, *Chem. Eur. J.*, 2011, **17**, 9560–9564.
13 (*a*) M. T. Whited, P. I. Djurovich, S. T. Roberts, A. C. Durrell, C. W. Schlenker, S. E. Bradforth, and M. E. Thompson, *J. Am. Chem. Soc.*, 2011, **133**, 88–96; (*b*) D. N. Kozhevnikov, V. N. Kozhevnikov, M. Z. Shafikov, A. M. Prokhorov, D. W. Bruce and J. A. Gareth Williams, *Inorg. Chem.*, 2011, **50**, 3804–3815; (*c*) S. M. Borisov, R. Saf, R. Fischer, and I. Klimant, *Inorg. Chem.*, 2013, **52**, 1206–1216; (*d*) Q. Zhao, C. Huang and F. Li, *Chem. Soc. Rev.*, 2011, **40**, 2508–2524.
14 J. Zhao, W. Wu, J. Sun and S. Guo, *Chem. Soc. Rev.*, 2013, **42**, 5323–5351.
15 J. Zhao, S. Ji, W. Wu, W. Wu, H. Guo, J. Sun, H. Sun, Y. Liu, Q. Li and L. Huang, *RSC Adv.*, 2012, **2**, 1712–1728.
16 (*a*) S. G. Awuahab and Y. You, *RSC Adv.*, 2012, **2**, 11169–11183; (*b*) N. Adarsh , R. Avirah , and D. Ramaiah, *Org. Lett.*, 2010, **12**, 5720–5723; (*c*) N. Adarsh, M. Shanmugasundaram, R. R. Avirah, and D. Ramaiah, *Chem.–Eur. J.* ,2012, **18**, 12655–12662.
17 C. Zhang, J. Zhao, S. Wu, Z. Wang, W. Wu, J. Ma, S. Guo, and L. Huang, *J. Am. Chem. Soc.*, 2013, **135**, 10566–10578.
18 S. Guo, L. Ma, J. Zhao, B. Küçüköz, A. Karatay, M. Hayvali, H. G. Yaglioglub and A. Elmalib, *Chem. Sci.*, 2014, **5**, 489–500.
19 J. Ma, X. Yuan, B. Küçüköz, S. Li, C. Zhang, P. Majumdar, A. Karatay, X. H. Li, H. G. Yaglioglu, A. Elmali, J. Zhao and M. Hayvali, *J. Mater. Chem. C*, 2014, **2**, 3900–3913.
20 W. Shi, R. Menting, E. A. Ermilov, P.-C. Lo, B. Röderb and D. P. Ng, *Chem. Commun.*, 2013, **49**, 5277–5279.
21 (*a*) T. Lazarides, G. Charalambidis, A. Vuillamy, M. Réglier, E. Klontzas, G. Froudakis, S. Kuhri, D. M. Guldi, and A. G. Coutsolelos, *Inorg. Chem.*, 2011, **50**, 8926–8936; (*b*) F. Hu, J. Huang, M. Cao, Z. Chen, Y. Yang, S. Liu and J. Yin, *Org. Biomol. Chem.*, 2014, **12**, 7712–7720; (*c*) K. Wang, C. Wang, Y. Zhang, S. Zhang, B. Yang and Y. Yang, *Chem. Commun.*, 2014, **50**, 9458–9461; (*d*) X. Hu, Z. Chen, L. Chen, L. Zhang, J. Hou and Z. Li, *Chem. Commun.*, 2012, 48, 10999–11001; (*e*) X. Xiao, N. Sun, D. Qi and J. Jiang, *Polym. Chem.*, 2014, **5**, 5211–5217; (f) J. P. Byrne, J. A. Kitchen and T. Gunnlaugsson, *Chem. Soc. Rev.*, 2014, **43**, 5302–5325.
22 (*a*) K. Feng, M. Yu, S. Wang, G. Wang, C. Tung and L. Wu, *ChemPhysChem.*, 2013, **14**, 198–203; (*b*) J. Yao, H. Li, Y. Xu, Q. Wang, D. Qu, *Chem. Asian J.*, 2014, 9, 3482–3490.
23 Á. J. Jiménez, R. M. K. Calderón, M. S. Rodríguez-Morgade, D. M. Guldi and T. Torres, *Chem. Sci.*, 2013, **4**, 1064–1074.
24 S. Gadde, D.-M. S. Islam, C. A. Wijesinghe, N. K. Subbaiyan, M. E. Zandler, Y. Araki, O. Ito, and F. D'Souza, *J. Phys. Chem. C.*, 2007, **111**, 12500–12503.
25 M. Segura , L. Sánchez, J. Mendoza, N. Martín, and D. M. Guldi, *J. Am. Chem. Soc.*, 2003, **125**, 15093–15100.
26 L. Sánchez, N. Martín, and D. M. Guldi, *Angew. Chem. Int. Ed.*, 2005, **44**, 5374–5382.
27 V. Nandwana, L. A. Serrano, K. M. Solntsev, B. Ebenhoch, Q. Liu, G. Y. Tonga, I. D. W. Samuel, G. Cooke, and V. M. Rotello, *Langmuir*, 2013, **29**, 7534–7537.
28 H. Fang, S. Wang, S. Xiao, J. Yang, Y. Li, Z. Shi, H. Li, H. Liu, S. Xiao, and D. Zhu, *Chem. Mater.*, 2003, **15**, 1593–1597.
29 Y. Liu, S. Xiao, H. Li, Y. Li, H. Liu, F. Lu, J. Zhuang, and D. Zhu, *J. Phys. Chem. B.*, 2004, **108**, 6256–6260.
30 J. W. Arbogast, A. P. Darmanyan, C. S. Foote, F. N. Diederich, R. L. Whetten , Y. Rubin, M. M. Alvarez, S. J. Anz, *J. Phys. Chem.*, 1991, **95**, 11–12.
31 C. Villegas, J. L. Delgado, P.-A. Bouit, B. Grimm, W. Seitz, N. Martín and D. M. Guldi, *Chem. Sci.*, 2011, **2**, 1677–1681.
32 A. N. Amin, M. E. El-Khouly, N. K. Subbaiyan, M. E. Zandler, S. C. Fukuzumi and F. D'Souza, *Chem. Commun.*, 2012, **48**, 206–208.
33 Y. Liu and J. Zhao, *Chem. Commun.*, 2012, **48**, 3751–3753.
34 R. Ziessel, B. D. Allen, D. B. Rewinska and A. Harriman, *Chem. Eur. J.*, 2009, **15**, 7382–7393.
35 W. Wu, J. Zhao, J. Sun and S. Guo. *J. Org. Chem.*, 2012, **77**, 5305–5312.
36 L. Huang, X. Yu, W. Wu and J. Zhao, *Org. lett.*, 2012, **14**, 2594–2597.
37 L. Huang, X. Cui, B. Therrien and J. Zhao, *Chem. Eur. J.*, 2013, **19**, 17472–17482.
38 G. Ulrich, R. Ziessel and A. Harriman, *Angew. Chem. Int. Ed.*, 2008, **47**, 1184–1201.
39 (*a*) H. Lu, J. Mack, Y. Yang and Z. Shen, *Chem. Soc. Rev.*, 2014, **43**, 4778–4823; (*b*) X. Yu, X. Jia, X. Yang, W. Liu and W. Qin, *RSC Adv.*, 2014, **4**, 23571-23579; (*c*) Y. Chen, H. Wang, L. Wan, Y. Bian and J. Jiang, *J. Org. Chem.*, 2011, **76**, 3774–3781.
40 A. Loudet and K. Burgess, *Chem. Rev.*, 2007, **107**, 4891–4932.
41 S. Erbas-Cakmak, O. A. Bozdemir, Y. Cakmak and E. U. Akkaya, *Chem. Sci.*, 2013, **4**, 858–862.
42 (*a*) O. A. Bozdemir, S. Erbas-Cakmak, O. O. Ekiz, A. Dana and E. U. Akkaya, *Angew. Chem. Int. Ed.*, 2011, **50**, 10907–10912; (*b*) C. Wan, A. Burghart, J. Chen, F. Bergström, L. Johansson, M. Wolford, T. GyumKim, M. Topp, R. Hochstrasser and K. Burgess, *Chem. Eur. J.* ,2003, **9**, 4430–4441.
43 D. Zhang, V. Martín, I. García-Moreno, A. Costela, M. E. Pérez-Ojedab and Y. Xiao, *Phys. Chem. Chem. Phys.*, 2011, **13**, 13026–13033.
44 J. R. Lakowicz, *Principles of Fluorescence Spectroscopy*, 2nd ed.; Kluwer Academic/Plenum Publishers: New York, 1999.
45 B. Valeur, *Molecular Fluorescence: Principles and Applications*; Wiley-VCH Verlag: GmbH, 2001.
46 A. Ghosh, A. Mandoli, D. K. Kumar, N. S. Yadav, T. Ghosh, B. Jha, J. A. Thomas and A. Das, *Dalton. Trans.*, 2009, **42**, 9312–9321.
47 Y. Chen, W. Lei, G. Jiang, Q. Zhou, Y. Hou, C. Li, B. Zhang and X. Wang, *Dalton. Trans.*, 2013, **42**, 5924–5931.
48 M. Urbani1, K. Ohkubo, D. M. S. Islam, S. Fukuzumi, and F. Langa1, *Chem. Eur. J.*, 2012, **18**, 7473–7485.
49 J. Liu, M. El-Khouly, S. Fukuzumi, and D. K. P. Ng, *Chem. Asian. J.*, 2011, **6**, 174–179.
50 M. E. El-Khouly and S. Fukuzumi, *J. Porphyrins. Phthalocyanines.*, 2011, **15**, 111–117.
51 C. C. Hofmann, S. M. Lindner, M. Ruppert, A. Hirsch, S. A. Haque, M. Thelakkat, and J. Köhler, *J. Phys. Chem. B.*, 2010, **114**, 9148–9156.

52 L. Zhang, B. Chen, L. Wu, C. Tung, H. Cao and Y. Tanimoto, *Chem. Eur. J.*, 2003, **9**, 2763–2769.
53 T. S. Balaban, N. Berova, C. M. Drain, R. Hauschild, X. F. Huang, H. Kalt, S. Lebedkin, J.-M. Lehn, F. Nifaitis, G. Pescitelli, V. I. Prokhorenko, G. Riedel, G. Smeureanu and J. Zeller, *Chem. Eur. J.*, 2007, **13**, 8411–8427.
54 C. V. Kumar, L. Qin, P. K. Das, *J. Chem. Soc. Faraday Trans.,* 2 1984, **80**, 783 –793.
55 J. Wang, P. Cieplak and P. A. Kollman, *J. Comput. Chem.*, 2000, **21**, 1049–1074
56 M. J. Frisch, G. W. Trucks, H. B. Schlegel, G. E. Scuseria, M. A. Robb, J. R. Cheeseman, G. Scalmani, V. Barone, B. Mennucci, G. A. Petersson, H. Nakatsuji, M. Caricato, X. Li, H. P. Hratchian, A. F. Izmaylov, J. Bloino, G. Zheng, J. L. Sonnenberg, M. Hada, M. Ehara, K. Toyota, R. Fukuda, J. Hasegawa, M. Ishida, T. Nakajima, Y. Honda, O. Kitao, H. Nakai, T. Vreven, J. A. Montgomery, Jr., J. E. Peralta, F. Ogliaro, M. Bearpark, J. J. Heyd, E. Brothers, K. N. Kudin, V. N. Staroverov, R. Kobayashi, J. Normand, K. Raghavachari, A. Rendell, J. C. Burant, S. S. Iyengar, J. Tomasi, M. Cossi, N. Rega, J. M. Millam, M. Klene, J. E. Knox, J. B. Cross, V. Bakken, C. Adamo, J. Jaramillo, R. Gomperts, R. E. Stratmann, O. Yazyev, A. J. Austin, R. Cammi, C. Pomelli, J. W. Ochterski, R. L. Martin, K. Morokuma, V. G. Zakrzewski, G. A. Voth, P. Salvador, J. J. Dannenberg, S. Dapprich, A. D. Daniels, O. Farkas, J. B. Foresman, J. V. Ortiz, J. Cioslowski, and D. J. Fox, *Gaussian 09, Revision A.01, Gaussian, Inc., Wallingford CT*, 2009.
57 W. Humphrey, A. Dalke and K. Schulten, *J. Mol. Graph.*, 1996, **14**, 33-8.
58 Z. Cao, Y. Peng, S. Li, L. Liu and T. Yan, *J. Phys. Chem. C.*, 2009, **113**, 3096–3104.
59 L. Monticelli, *J. Chem. Theory. Comput.*, 2012, **8**, 1370–1378.
60 A. D. MacKerell, Jr, D. Bashford, M. Bellott , R. L. Dunbrack, Jr., J. D. Evanseck, M. J. Field, S. Fischer, J. Gao, H. Guo, S. Ha, D. Joseph-McCarthy, L. Kuchnir, K. Kuczera, F. T. K. Lau, C. Mattos, S. Michnick, T. Ngo, D. T. Nguyen, B. Prodhom, W. E. Reiher, B. Roux, M. Schlenkrich, J. C. Smith, R. Stote, J. Straub, M. Watanabe, J. Wiórkiewicz-Kuczera, D. Yin, and M. Karplus, *J. Phys. Chem. B.*, 1998, **102**, 3586–3616.
61 J. C. Phillips, R. Braun, W. Wang, J. Gumbart, E. Tajkhorshid, E. Villa1, C Chipot, R. D. Skeel, L. Kalé and K. Schulten. *J. Comput. Chem.*, 2005, **26**, 1781–1802.